Multiplicity of the doubly charmed state T_{cc}^{+} in heavy-ion collisions

L. M. Abreu* and H. P. L. Vieira†
Instituto de Física, Universidade Federal da Bahia, Campus Universitário de Ondina, 40170-115 Bahia, Brazil

F. S. Navarra‡
Instituto de Física, Universidade de São Paulo, Rua do Matão, 1371 CEP 05508-090 São Paulo, SP, Brazil

(Received 2 March 2022; accepted 23 June 2022; published 30 June 2022)

We study the evolution of the doubly charmed state T_{cc}^{+} in a hot hadron gas produced in the late stage of heavy-ion collisions. We use effective Lagrangians to calculate the thermally averaged cross sections of T_{cc}^{+} production in reactions such as $D^{(*)}D^{(*)} \to T_{cc}^{+}\pi, T_{cc}^{+}\rho$ and its absorption in the corresponding inverse processes. We then solve the rate equation to follow the time evolution of the T_{cc}^{+} multiplicity and determine how it is affected by the considered reactions during the expansion of the hadronic matter. We compare the evolution of the T_{cc}^{+} abundance treated as a hadronic S-wave molecule and as a tetraquark state. Our results show that the tetraquark yield increases by a factor of about 2 at freeze-out, but it is still almost 2 orders of magnitude smaller than the final yield of molecules formed from hadron coalescence. We also analyze the dependence of the yields with the system size, represented by $\mathcal{N} = [dN_{ch}/d\eta(\eta < 0.5)]^{1/3}$. We make predictions that can be confronted with data, when they are available.

DOI: 10.1103/PhysRevD.105.116029

I. INTRODUCTION

The LHCb Collaboration reported a few months ago the observation of the first doubly charmed tetraquark state in proton-proton (pp) collisions, with statistical significance of more than 10σ [1,2]. It has been identified from the fit of a narrow peak seen in the $D^0D^0\pi^+$-mass spectrum to one resonance with a mass of approximately 3875 MeV and quantum numbers $J^P = 1^+$. Its minimum valence quark content is $cc\bar{u}\bar{d}$. From the data, the binding energy with respect to the $D^{*+}D^0$ mass threshold and the decay width are estimated to be $273 \pm 61 \pm 5^{+11}_{-14}$ keV and $410 \pm 165 \pm 43^{+18}_{-38}$ keV, respectively, which are consistent with the expected properties of a T_{cc}^{+} isoscalar tetraquark ground state with $J^P = 1^+$ [3–14]. Since its detection, many works appeared debating the possible mechanisms of its decay/formation and trying to answer the question of whether it is an extended hadron molecule or a compact tetraquark [15–30].

To reach a more complete picture of the T_{cc}^{+} state, additional experimental and theoretical work is needed. In this sense, in Ref. [28], we have suggested that a good environment to study the T_{cc}^{+} properties is the one provided by heavy ion collisions (HIC), where a large number of charm quarks is produced. In a typical HIC, there is a phase transition from nuclear matter to the locally thermalized state of deconfined quarks and gluons—the so-called quark-gluon plasma (QGP), which expands, cools down, and becomes a gas of hadrons. In this last transition, heavy quarks coalesce to form multiquark bound states. As the hadronic phase evolves, the multiquark states interact with other hadrons, being destroyed in collisions with the comoving light mesons or produced through the inverse processes [31–39]. At this stage, the spatial configuration of the multiquark systems influences the hadronic interactions and therefore, the final yields. More concretely: similarly to the $X(3872)$ state (see the discussion in Ref. [34]), charm meson molecules DD^* are larger than charm tetraquarks in a diquark-antidiquark configuration $(cc) - (\bar{q}\bar{q})$ by a factor about 3–10, and therefore, their absorption cross sections may be 1 order of magnitude larger. In contrast, when the T_{cc} is produced from $D - D^*$ fusion in a hadron gas, the initial $D + D^*$ state has a bigger spatial overlap with a molecule than with a tetraquark. For this reason, molecules are expected to be more easily produced as well as more easily destroyed than compact tetraquarks in a hot hadronic environment.

*luciano.abreu@ufba.br
†hildeson.paulo@ufba.br
‡navarra@if.usp.br

To the best of our knowledge, the interactions of the T_{cc} in a hadronic medium were first discussed in Ref. [11] (published before the observation of the T_{cc} by the LHCb Collaboration). The T_{cc} was treated as an extremely shallow bound state of a D and a D^*. The authors used the quasifree approximation, in which the charm mesons are understood to be on shell and their binding energy and mutual interaction are neglected. In this approximation, the T_{cc} is absorbed when a pion from the hadron gas interacts with the D or with the D^*. In this approach, the dynamical component needed is just the effective $D^*D\pi$ Lagrangian. The results suggested that the hadronic effects on the T_{cc} final abundance depend on the initial yield of T_{cc} produced from the quark-gluon plasma phase, which is determined by the assumed structure of the state.

We believe that the subject deserves further discussion. In a recent paper [28], we computed the cross sections of T_{cc} production in reactions such as $D^{(*)}D^{(*)} \to T_{cc}\pi, T_{cc}\rho$ and its absorption in the corresponding inverse processes. The absorption cross sections were found to be larger than the production ones. These results were obtained using effective field Lagrangians to account for the couplings between light and heavy mesons. For the new state, there is no Lagrangian, and we had to study the $T_{cc} - D - D^*$ with QCD sum rules, determining, for the first time, the form factor and the coupling constant.

In Ref. [28], the time evolution of the T_{cc} abundance in the hot hadron gas was not addressed. Thus, in this work, we complete the work done in Ref. [28]. We calculate the thermally averaged cross sections of T_{cc}^+ production and absorption, and use them as input to solve the kinetic equation and obtain the time evolution of the T_{cc}^+ multiplicity. We compute the T_{cc}^+ abundance considering it as a hadronic molecule and also as a tetraquark state and compare them. Also, we present a comparison between the time evolution of the multiplicities of T_{cc} and of $X(3872)$ in similar conditions. We finish with a discussion on the dependence of the ratio $R = N_{T_{cc}}/N_{X(3872)}$ with the multiplicity density of charged particles measured at midrapidity $\mathcal{N} = [dN_{ch}/d\eta(\eta < 0.5)]^{1/3}$.

The paper is organized as follows. In Sec. II, we discuss the cross sections averaged over the thermal distributions. In Sec. III, we investigate the time evolution of the $X(3872)$ abundance by solving the kinetic equation. Finally, Sec. V is devoted to the summary and to the concluding remarks.

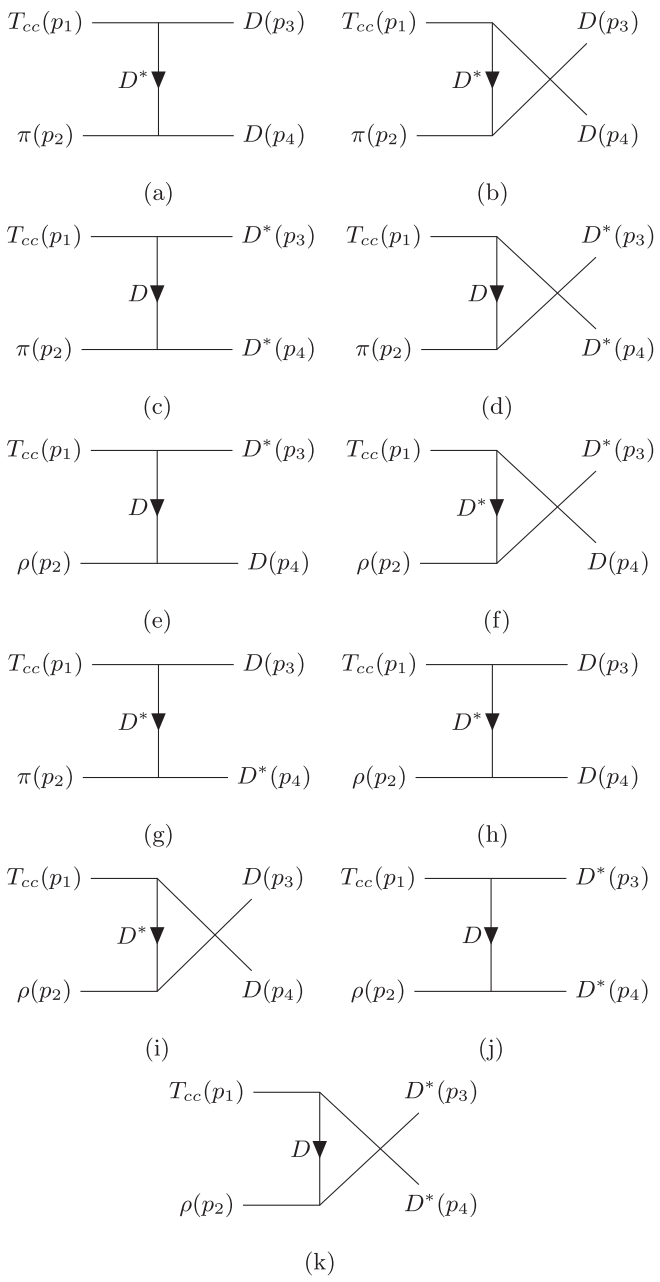

FIG. 1. Reproduction of Born diagrams treated in Ref. [28] contributing to the following process (without specification of the charges of the particles): $T_{cc}\pi \to DD$ [(a) and (b)], $T_{cc}\pi \to D^*D^*$ [(c) and (d)], $T_{cc}\rho \to D^*D$ [(e) and (f)], $T_{cc}\pi \to DD^*$ [(g)], $T_{cc}\rho \to DD$ [(h) and (i)], and $T_{cc}\rho \to D^*D^*$ [(j) and (k)]. The particle charges are not specified.

II. CROSS SECTIONS AVERAGED OVER THE THERMAL DISTRIBUTIONS

We are interested in the hadronic effects on the T_{cc}^+ state in a heavy-ion collision environment, in particular, in how its multiplicity is affected by the production and absorption reactions during the expansion of the hadron gas. The interactions of T_{cc}^+ with other hadrons are described with the help of the results reported in our previous work [28], especially focusing on the reactions $T_{cc}^+\pi \to D^{(*)}D^{(*)}$ and $T_{cc}^+\rho \to D^{(*)}D^{(*)}$, as well as the corresponding inverse processes. We reproduce the lowest-order Born diagrams considered in Fig. 1. In the diagrams 1(a)–1(f), the vertices involving light and heavy-light mesons are described by effective Lagrangians of the type $\mathcal{L}_{PPV}$ and $\mathcal{L}_{VVV}$, where P and V are pseudoscalar and vector mesons, respectively. In the case of the diagrams 1(g)–1(k), the vertices involving

light and heavy-light mesons are anomalous; i.e., they must be of the type $\mathcal{L}_{PVV}$ [28]. Taking into consideration that the T_{cc}^{+} has quantum numbers $I(J^P) = 0(1^+)$, its effective coupling with the DD^* pair is of the form $\mathcal{L}_{T_{cc}} = ig_{T_{cc}DD^*}T_{cc}^{\mu}D_{\mu}^{*}D$ [23,28], where T_{cc} denotes the field associated to T_{cc}^{+} state; this notation will be used in what follows. Also, the $D_{\mu}^{*}D$ represents the $D_{\mu}^{*+}D^0$ and $D_{\mu}^{*0}D^+$ components, although we do not distinguish them here since we will use isospin-averaged masses. As mentioned above, in [28], we have determined the form factor and the corresponding coupling constant associated to the $T_{cc} - D - D^*$ vertex with QCD sum rules (QCDSR). A comprehensive study on the T_{cc} cross sections has been performed.

All the aforementioned reactions happen in a hadron gas at finite temperature, which should drive the collision energies of the colliding particles. As a consequence, the relevant dynamical quantity is the cross section averaged over the thermal distribution for a reaction involving an initial two-particle state going into two final particles $ab \to cd$. It is defined as [32,34,40]

$$\begin{aligned}\langle \sigma_{ab\to cd} v_{ab} \rangle &= \frac{\int d^3\mathbf{p}_a d^3\mathbf{p}_b f_a(\mathbf{p}_a) f_b(\mathbf{p}_b) \sigma_{ab\to cd} v_{ab}}{\int d^3\mathbf{p}_a d^3\mathbf{p}_b f_a(\mathbf{p}_a) f_b(\mathbf{p}_b)} \\ &= \frac{1}{4\alpha_a^2 K_2(\alpha_a)\alpha_b^2 K_2(\alpha_b)} \int_{z_0}^{\infty} dz K_1(z) \\ &\quad \times \sigma(s = z^2T^2)[z^2 - (\alpha_a + \alpha_b)^2] \\ &\quad \times [z^2 - (\alpha_a - \alpha_b)^2], \end{aligned} \tag{1}$$

where v_{ab} represents the relative velocity of the two initial interacting particles a and b; $\sigma_{ab\to cd}$ denotes the cross sections evaluated in [28] for the different reactions shown in Fig. 1; the function $f_i(\mathbf{p}_i)$ is the Bose-Einstein distribution of particles of species i, which depends on the temperature T; $\beta_i = m_i/T$, $z_0 = \max(\beta_a + \beta_b, \beta_c + \beta_d)$; and K_1 and K_2 the modified Bessel functions.

In Figs. 2 and 3, we plot the thermally averaged cross sections as functions of the temperature for T_{cc} absorption and production, respectively, via the processes discussed above. The bands in the figures express the uncertainty in the coupling constant $g_{T_{cc}DD^*}$ coming from variations in the quantities relevant in the QCDSR calculations [28]. It can be seen that, in general, the reactions involving a pion in initial or final state have greater thermal cross sections than those with a ρ meson. Interestingly, the thermal cross sections $\langle \sigma_{ab\to cd} v_{ab} \rangle$ for T_{cc} absorption do not change appreciably in the considered range of temperature (remaining almost constant), when compared to corresponding ones for the T_{cc} production. Also, the results suggest that the channels $T_{cc}\pi \to DD, DD^*$ have similar magnitudes, with the final state D^*D^* being enhanced with respect to these other ones by almost 2 orders of magnitude. On the other hand, considering the uncertainty, the

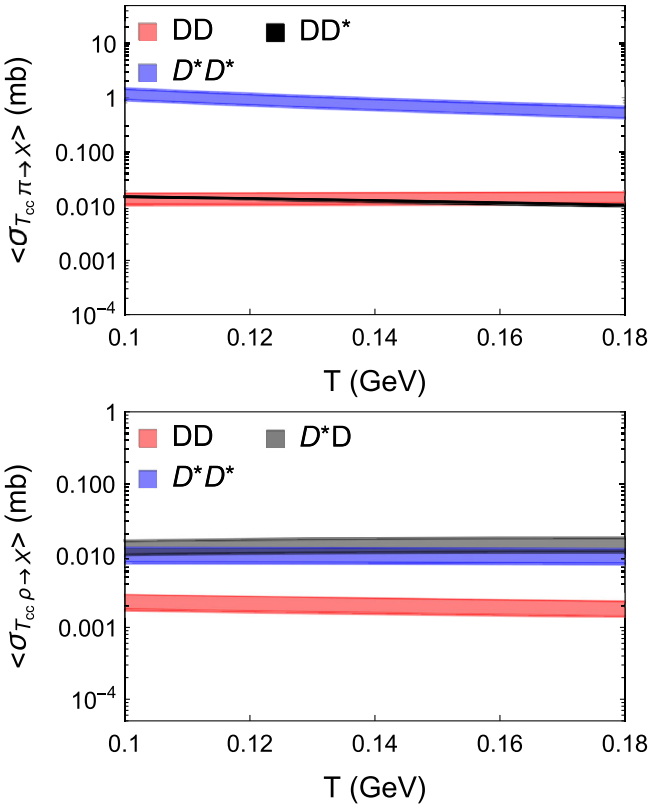

FIG. 2. Thermally averaged cross sections for the absorption processes $T_{cc}^{+}\pi \to D^{(*)}D^{(*)}$ (top panel) and $T_{cc}^{+}\rho \to D^{(*)}D^{(*)}$ (bottom panel), as a function of temperature T. Upper and lower limits of the bands are obtained taking the upper and lower limits of the uncertainty in the coupling constant $g_{T_{cc}DD^*}$ [28]. In the top panel, the band for the DD and DD^* channels coincide.

channels for $T_{cc}\rho \to DD^*, D^*D^*$ have similar magnitudes, whereas the final state $T_{cc}\rho \to DD$ is smaller by almost 1 order of magnitude.

The most important conclusion from these figures is that the thermally averaged cross sections for T_{cc} annihilation are bigger than those for production, at least by 1 or 2 orders of magnitude. This might play an important role in the time evolution of the T_{cc} multiplicity. Thus, in the next section, we use these thermally averaged cross sections as input in the rate equation and study the time evolution of the doubly charmed state abundance.

We would like to close this section with a comparison between our findings and those reported in Ref. [11]. In the approach developed on [11], the T_{cc} is absorbed when a pion from the hadron gas interacts either with the D or with the D^*. In each of these interactions, the other heavy meson is a spectator. As discussed in Ref. [28], this approach has the advantage of relying solely on the well-known $D^*D\pi$ Lagrangian. However, it ignores the possible dynamical effects associated with the quantum numbers of the D^*D bound state. Moreover, it does not include some possible final states. We remember that, as pointed out in Ref. [28],

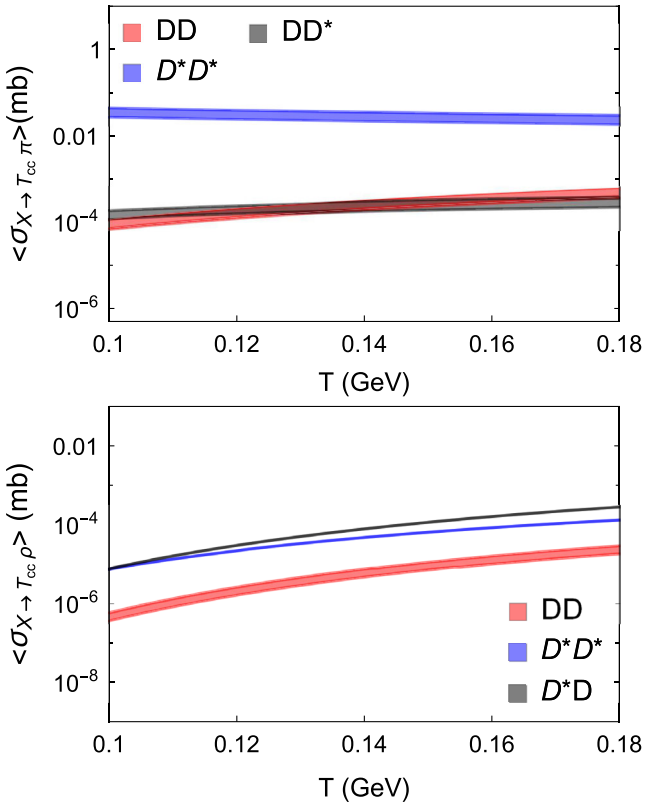

FIG. 3. Thermally averaged cross sections as a function of temperature for the respective inverse (production) processes displayed in Fig. 1, i.e., $D^{(*)}D^{(*)} \to T_{cc}^{+}\pi$ (top panel) and $D^{(*)}D^{(*)} \to T_{cc}^{+}\rho$ (bottom panel), obtained via the detailed balance relation. Upper and lower limits of the bands are obtained taking the upper and lower limits of the uncertainty in the coupling constant $g_{T_{cc}DD^*}$ [28].

the cross sections for the absorption of the T_{cc} by pions in the quasifree approximation are much larger than those obtained with the present approach. For completeness, we show in Fig. 4 the thermal cross section for the T_{cc} absorption by pions in the quasifree approximation. As expected, it is much larger than the one shown in Fig. 2.

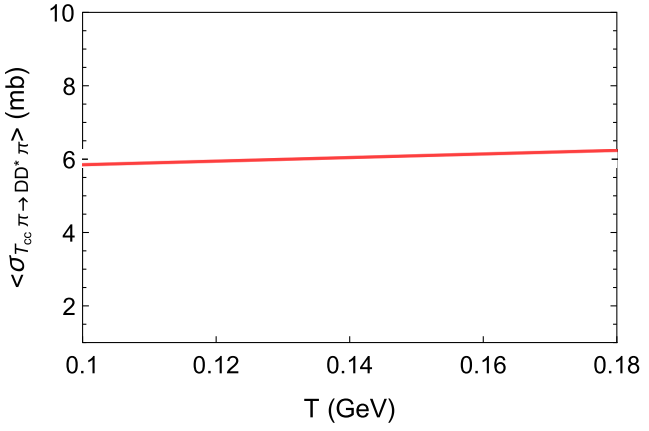

FIG. 4. Thermal cross sections as a function of the temperature for the T_{cc} absorption by pions in the quasifree approximation, which, according to Eq. (26) of Ref. [11], is given by $\langle\sigma_{T_{cc}\pi\to DD^*\pi} v_{T_{cc}\pi}\rangle = \langle\sigma_{D\pi\to D\pi} v_{T_{cc}\pi}\rangle + \langle\sigma_{D^*\pi\to D^*\pi} v_{T_{cc}\pi}\rangle$.

III. TIME EVOLUTION OF THE T_{cc}^{+} ABUNDANCE

A. The rate equation

Now we study the effect of the $\pi(\rho) - T_{cc}$ interactions on the abundance of T_{cc}^{+} during the hadron gas phase of heavy ion collisions. The momentum-integrated evolution equation for the T_{cc} abundance reads [32,34,40]

$$\frac{dN_{T_{cc}}(\tau)}{d\tau} = \sum_{\substack{c,c'=D,D^* \\ \varphi=\pi,\rho}} [\langle\sigma_{cc'\to T_{cc}\varphi} v_{cc'}\rangle n_c(\tau) N_{c'}(\tau) - \langle\sigma_{\varphi T_{cc}\to cc'} v_{T_{cc}\varphi}\rangle n_\varphi(\tau) N_{T_{cc}}(\tau)], \quad (2)$$

where $N_{T_{cc}}(\tau)$, $N_{c'}(\tau)$, $n_c(\tau)$, and $n_\varphi(\tau)$ are the abundances of T_{cc} and of charmed mesons of type c', and the densities of charmed mesons of type c and of light mesons at proper time τ, respectively. Equation (2) implies that the time evolution of $N_{T_{cc}}(\tau)$ depends on both the T_{cc} dissociation and production rates through the processes discussed previously.

To solve Eq. (2), we assume that the pions, ρ, and charmed mesons in the reactions contributing to the abundance of T_{cc} are in equilibrium. Accordingly, $n_c(\tau)$, $N_{c'}(\tau)$ and $n_\varphi(\tau)$ can be written as [32,34,40]

$$n_i(\tau) \approx \frac{1}{2\pi^2}\gamma_i g_i m_i^2 T(\tau) K_2\left(\frac{m_i}{T(\tau)}\right), \quad (3)$$

where γ_i and g_i are the fugacity factor, the degeneracy factor and m_i the mass of the particle i, respectively. The multiplicity $N_i(\tau)$ is obtained by multiplying the density $n_i(\tau)$ by the volume $V(\tau)$.

The time dependence of the density $n_i(\tau)$ is encoded in the parametrization of the temperature $T(\tau)$ and of the volume $V(\tau)$, which are fitted to reproduce the properties of the hadron gas. According to the boost invariant Bjorken picture, the hydrodynamical expansion and cooling of the hadron gas is modeled as an accelerated transverse expansion [32,34,40], by the expressions (for $\tau \geq \tau_H$),

$$V(\tau) = \pi\left[R_C + v_C(\tau - \tau_C) + \frac{a_C}{2}(\tau - \tau_C)^2\right]^2 \tau_C,$$
$$T(\tau) = T_C - (T_H - T_F)\left(\frac{\tau - \tau_H}{\tau_F - \tau_H}\right)^{\frac{4}{5}}, \quad (4)$$

where R_C and τ_C denote the final transverse and longitudinal sizes of the QGP; v_C and a_C are its transverse flow

velocity and transverse acceleration at τ_C; T_C is the critical temperature of the quark-hadron phase transition; T_H is the temperature of the hadronic matter at the end of the mixed phase, occurring at the time τ_H; and the kinetic freeze-out occurs at τ_F, when the temperature is T_F. We emphasize that this parametrization is employed as a proxy for capturing the basic elements of hydrodynamic expansion and cooling of the hadron matter, being adequate for our phenomenological approach, keeping in mind that our focus is on the behavior of the T_{cc} multiplicity during the evolution of hadron gas phase. For a discussion of the features and limitations of this model, we refer the reader to Ref. [41]. A more realistic hydrodynamical simulation is postponed to subsequent works.

B. The initial conditions

Unless explicitly stated otherwise, all the results refer to the hadronic medium produced in central $Pb-Pb$ collisions at $\sqrt{s_{NN}} = 5.02$ TeV at the LHC. We use in Eq. (4) the set of parameters of Ref. [42], which has been obtained in order to reproduce the quantities listed in Table 3.1 of Ref. [43]. The values of these parameters are given in Table I. We assume that the total number of charm quarks (N_c) in charmed hadrons is conserved during the production and dissociation reactions, i.e., $n_c(\tau) \times V(\tau) = N_c = \text{const}$. By doing this, the charm quark fugacity factor γ_c in Eq. (3) is assumed to be time dependent. In the case of pions and ρ mesons, their fugacities appear as normalization parameters, adjusted to fit the multiplicities given in Table I. We consider the yields obtained for the T_{cc} with the coalescence model. In this model, the yield of a hadronic state depends on the overlap of the density matrix of its constituents with its Wigner function. Consequently, this model encodes essential features of the internal structure, such as angular momentum, number of constituent quarks, etc. Accordingly, the T_{cc} multiplicity at the end of the quark-gluon plasma phase is given by [32,34,42,43]

TABLE I. Set of parameters used in Eq. (4) for the hydrodynamic expansion and cooling of the hadronic medium formed in central $Pb-Pb$ collisions at $\sqrt{s_{NN}} = 5.02$ TeV [42,43].

v_C (c)	a_C (c^2/fm)	R_C (fm)
0.5	0.09	11
τ_C (fm/c)	τ_H (fm/c)	τ_F (fm/c)
7.1	10.2	21.5
T_C(MeV)	T_H(MeV)	T_F(MeV)
156	156	115
N_c	$N_\pi(\tau_F)$	$N_\rho(\tau_H)$
14	2410	184
V_C (fm^3)		
5380		

$$N_{T_{cc}}^{Coal} \approx g_{T_{cc}} \prod_{j=1}^{n} \frac{N_j}{g_j} \prod_{i=1}^{n-1} \frac{(4\pi\sigma_i^2)^{\frac{3}{2}}}{V(1+2\mu_i T\sigma_i^2)} \times \left[\frac{4\mu_i T\sigma_i^2}{3(1+2\mu_i T\sigma_i^2)}\right]^{l_i}, \quad (5)$$

where g_j and N_j are the degeneracy and number of the jth constituent of the T_{cc} and $\sigma_i = (\mu_i\omega)^{-1/2}$. The quantity ω is the oscillator frequency (taking an harmonic oscillator as a picture for the hadron internal structure), and μ the reduced mass, i.e., $\mu^{-1} = m_{i+1}^{-1} + (\sum_{j=1}^{i} m_j)^{-1}$. The angular momentum of the system, l_i, is 0 for an S wave, and 1 for a P wave. According to the coalescence model, the T_{cc} is produced as a S-wave tetraquark produced at the end of the QGP phase at the critical temperature, when the volume is V_C. The oscillator frequency for tetraquark states produced via quark coalescence mechanism, and the quark masses have been taken to be $\omega_c = 220$ MeV and $m_q = 350$ MeV, $m_c = 1500$ MeV, respectively [43]. For molecular states, to calculate the oscillation frequency, we have employed the expression $\omega = 6B$, with B being the binding energy. In Table II, we give the multiplicities. For the sake of comparison, we have also included the multiplicities calculated for the state $X(3872)$. We have used in Eq. (5) the fact that if there are N_c charm and N_c anticharm quarks in a given event, then we can form a total of $N_c(N_c-1)/2$ cc pairs ($\approx N_c^2/2$ for $N_c \gg 1$) and N_c^2 $c\bar{c}$ pairs. In contrast, in the case of $N_{T_{cc}}^{(Mol)}$ and $N_{X(3872)}^{(Mol)}$, we have yields of the same order for both DD^* and $D\bar{D}^*$ pairs [27]; the difference comes from ω.

As discussed in the previous section, to estimate the T_{cc} production and absorption contributions, we are using the form factors and couplings calculated with QCDSR, which are more appropriate to multiquark systems in a compact configuration. Indeed, in the three-point correlation function in the QCDSR calculation, all the quark fields in the current are defined at the same space-time point (we refer the reader to Ref. [28] for a more detailed discussion).

C. The T_{cc} and $X(3872)$ abundances

Now we study the time evolution of the T_{cc} abundance by solving Eq. (2), with initial conditions computed with the coalescence model and given in Table II. In the tetraquark configuration, the T_{cc} is a compact object and

TABLE II. The T_{cc} yields in central $Pb-Pb$ collisions at $\sqrt{s_{NN}} = 5.02$ TeV at the LHC using the coalescence model, Eq. (5), for compact tetraquark ($4q$) and for molecular (Mol) configurations.

State	$N^{(4q)}(\tau_C)$	$N^{(Mol)}(\tau_H)$
T_{cc}^+	8.40×10^{-5}	4.10×10^{-2}
$X(3872)$	1.81×10^{-4}	7.50×10^{-2}

its coupling constants and form factors can be computed with QCDSR, as discussed in detail in [28]. In the molecular configuration, it is a very weakly bound state, and its interaction cross sections can be computed with the model proposed in Ref. [11]. In this model, the authors make use of the "quasifree" approximation. The D and the D^*, which form the T_{cc}, are treated as approximately free particles that can interact with the pions and ρ's of the environment. The composite system is so weakly bound that any of these interactions is able to destroy the T_{cc}.

In Fig. 5(a), we show the time evolution of the T_{cc} abundance as a function of the proper time. In the tetraquark curve, the band represents the uncertainties coming from the QCDSR calculations of the absorption and production cross sections [28]. In the figure, we observe a strong sensitivity to the initial yields. This can be understood looking at the two terms on the right side of the rate equation (2): the first, positive, is the "gain" term, whereas the second, negative, is the "loss" term, which depends on $N_{T_{cc}}$. When $N_{T_{cc}}$ is initially very small (as it is for tetraquarks), the second term is very small, the first term dominates, the derivative $dN_{T_{cc}}/d\tau$ is positive and the abundance of T_{cc} increases. When $N_{T_{cc}}$ is initially large, the second term is bigger than the first, the derivative $dN_{T_{cc}}/d\tau$ is negative, and the abundance of T_{cc} decreases. We conclude that, for tetraquarks, $N_{T_{cc}}^{(4q)}$ increases by a factor of $\simeq 2$ during the hadron gas phase. For molecules, the absorption and regeneration terms yield similar contributions, with the predominance of the former and $N_{T_{cc}}^{(Mol)}$ decreases. Comparing the final yields $N_{T_{cc}}^{(4q)}(\tau_F)$ and $N_{T_{cc}}^{(Mol)}(\tau_F)$, shown in Fig. 5(a), we find that for the molecular configuration the number of T_{cc}'s at the end of the hadron gas phase is 2 orders of magnitude larger. The difference in multiplicities decreases during the hadron gas phase but it is still large at the end of the collision.

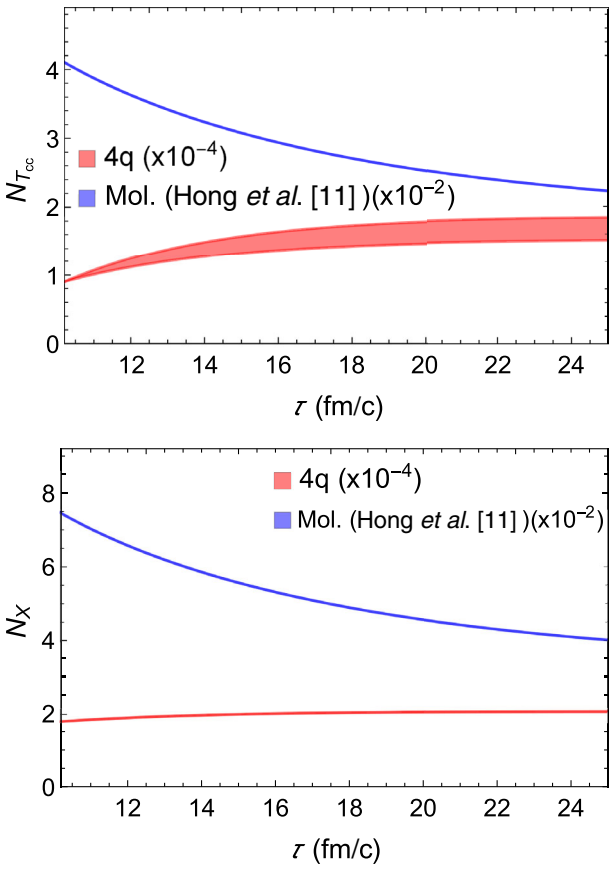

FIG. 5. (a) Time evolution of the T_{cc} abundance as a function of the proper time in central $Pb-Pb$ collisions at $\sqrt{s_{NN}}=5.02$ TeV, with initial conditions given by the coalescence model. The tetraquark and molecular abundances have been obtained from the present approach (red curve), and from that described in Ref. [11] (blue curve). (b) Same as (a) but for the $X(3872)$ state.

For the sake of comparison in Fig. 5(b), we show a plot similar to the one in Fig. 5(a) but for the $X(3872)$ state. We remark that the time evolution of $N_{X(3872)}$ has already been analyzed in Refs. [32,34], but in both cases, the HIC environment chosen has been the central $Au-Au$ collisions at $\sqrt{s_{NN}}=200$ GeV at RHIC. In order to make a fair comparison between the T_{cc} and $X(3872)$ yields, we have redone the calculations of Refs. [32,34] using the analogous reaction mechanisms for both states. As already mentioned above, the form factors in the vertices of the T_{cc} reactions have been calculated with QCD sum rules. Unfortunately, the equivalent vertices for the $X(3872)$ are not available in QCDSR. Thus, in this latter case, we have followed [32,34] and used empirical monopole form factors taking the cutoff $\Lambda=2.0$ GeV.

In the present calculation of the tetraquark cross sections and time evolution, we have ignored the terms with anomalous couplings, both in the $X(3872)$ and T_{cc} interactions. This is because the required coupling $T_{cc}D^*D^*$ is not yet available, and its computation is beyond the scope of the present work. We are using the model of [11] for the molecules, and in this model, the coupling $T_{cc}D^*D^*$ does not exist. Therefore, molecules are not affected by the lack of the anomalous couplings, only tetraquarks. The similarities in mass and quantum numbers between $X(3872)$ and T_{cc} suggest that the inclusion of the anomalous couplings interactions would reduce the multiplicity of tetraquark T_{cc}'s as it did for the $X(3872)$ (see Ref. [34]). The procedure adopted here allows for a fair comparison between $X(3872)$ and T_{cc} tetraquarks. However, because of the approximations involved, our results should be regarded as upper limits for the multiplicities.

To summarize: using QCDSR and the quasifree model, we are able to perform a fair comparison between the tetraquark (with both tetraquark initial conditions and cross sections) and molecular (with both molecular initial conditions and cross sections) approaches. We observe that if the T_{cc} is a molecule, it will be produced more abundantly

than a tetraquark, and its multiplicity will decrease with time. In contrast, tetraquarks would be produced much less abundantly, and their multiplicity would grow with time. The difference in multiplicities decreases during the hadron gas phase, but it is still large at the end of the collision. We conclude that molecules will be much more abundant (by a factor 100) than tetraquarks. This is in qualitative agreement with the results found in [11]. The results for the $X(3872)$ are quite similar and indicate that, even after going through the hadron gas phase, molecules remain much more abundant than tetraquarks.

IV. SYSTEM SIZE DEPENDENCE

Now we focus on the dependence of our results with the system size, represented here by the density of charged particles measured at midrapidity $\mathcal{N} = [dN_{ch}/d\eta(|\eta| < 0.5)]^{1/3}$. In our calculation, we need to take into account the dependence of all the relevant quantities with the charged particle multiplicity. As it can be seen from Eq. (5), the initial number of T_{cc} tetraquarks depends on N_c and on the volume V_C. The initial number of T_{cc} molecules depends on N_D and on the volume V_H. All these quantities depend on the system size, $\mathcal{N}$. The advantage of expressing the multiplicities in terms of $\mathcal{N}$, instead of τ, is that the former is a measurable quantity. In what follows, we explain how we can incorporate this dependence in our formalism.

A. Kinetic freeze-out time and temperature

As discussed in Ref. [39], $\mathcal{N}$ may be empirically related to the kinetic freeze-out temperature via the expression,

$$T_F = T_{F0} e^{-b\mathcal{N}}, \tag{6}$$

where T_{F0} and b are constants chosen in order to fit the results of the blast wave model analysis of the data performed by the ALICE Collaboration in [44]. The freeze-out temperature depends on the system size. This is not surprising and has been realized long ago [45]. The values used here are the same of [39]: $T_{F0} = 132.5$ MeV and $b = 0.02$. Assuming that the hadron gas undergoes a Bjorken-like cooling, the freeze-out time, τ_F, can be related to the freeze-out temperature, T_F, through the expression,

$$\tau_F = \tau_H \left(\frac{T_H}{T_F}\right)^3. \tag{7}$$

Inserting Eq. (6) into the above relation, we find:

$$\tau_F = \tau_H \left(\frac{T_H}{T_{F0}}\right)^3 e^{3b\mathcal{N}}. \tag{8}$$

With the above expression, from the observable quantity $\mathcal{N}$, we can infer the duration of the hadronic phase. As it can be seen, larger systems produce more particles, a larger $\mathcal{N}$, and live longer. Hence, the use of Eq. (8) in the solutions of Eq. (2) allows us to calculate $N_{T_{cc}}$ and $N_{X(3872)}$ as a function $\mathcal{N}$.

B. The volume

In Ref. [46], the authors used the statistical hadronization model (SHM) to perform an extensive fit of several hadron yields measured by the ALICE Collaboration in different centrality bins, at different energies, and in $p-p$, $p-Pb$, and $Pb-Pb$ collisions. In their Fig. 4, they present the relation between the volume per rapidity slice, dV/dy, and the central multiplicity density, $dN_{ch}/d\eta$, which they parametrize as

$$\frac{dV}{dy} = 2.4 \frac{dN_{ch}}{d\eta}(|\eta| < 0.5) = 2.4\mathcal{N}^3.$$

Integrating this equation over the appropriate rapidity interval, we find $V = \text{const}\mathcal{N}^3$. The constant can be determined by imposing that $V = 5380$ fm^3* when $\mathcal{N} \approx 12.43$ (and $[dN_{ch}/d\eta(\eta < 0.5)] = 1908$ [47]). We finally obtain

$$V = 2.82\mathcal{N}^3. \tag{9}$$

In the context of the SHM, V is the chemical freeze-out volume. Here, we will follow Ref. [43] and assume that $V = V_H = V_C$.

C. The number of charm quarks

As far as we can tell, there is no experimentally established connection between N_c and $dN_{ch}/d\eta(\eta < 0.5)$. We will make use of the only work where this relation was studied. In [48], the ALICE Collaboration measured the production of charm mesons in pp collisions at $\sqrt{s} = 7$ TeV. In the Fig. 2 of that paper, there is plot of the differential distribution of D mesons as a function of $dN_{ch}/d\eta$. The experimental points can be parametrized by a power law,

$$\frac{d^2N_D}{dydp_T} \Big/ \left\langle \frac{d^2N}{dydp_T} \right\rangle = \alpha' \left(\frac{dN_{ch}}{d\eta} \Big/ \left\langle \frac{dN_{ch}}{d\eta} \right\rangle \right)^{\beta},$$

where the quantities in brackets are average values. Fitting the experimental points, we find that $\beta = 1.6$. Integrating over the appropriate interval of rapidity and transverse momentum and rearranging the constants, we arrive at

$$N_D = \alpha'' \left(\frac{dN_{ch}}{d\eta}\right)^{\beta} = \alpha''(\mathcal{N}^3)^{\beta}. \tag{10}$$

We further assume that the number of charm quarks and the number of D mesons are proportional,

$$N_c = \text{const.} N_D = \alpha(\mathcal{N}^3)^{\beta}. \tag{11}$$

The constant α can be determined by using the numbers shown in Table I. In particular, we must have $N_c = 14$ for $\mathcal{N} = 12.43$. We finally arrive at

$$N_c = 7.9 \times 10^{-5} \mathcal{N}^{4.8}. \tag{12}$$

Having established relations between the relevant quantities and $\mathcal{N}$, we proceed as follows. We first choose the system size parameter, $\mathcal{N}$. Then, substituting (9), (10), and (12) into (5), we obtain the $\mathcal{N}$ dependent initial conditions. In the coalescence model, the number of composite particles depends on the volume. This dependence is very different if the number of constituents is two (molecules) or four (tetraquarks). Indeed, from (5), we have $N^{mol} \propto 1/V$ and $N^{4q} \propto 1/V^3$. The number of available charm quarks or D mesons also depends on the volume of the system. However, as we can see from (11), this dependence will be the same for molecules and tetraquarks. With the above mentioned substitutions we arrive at

$$N^{4q} \propto \mathcal{N}^{0.6} \quad \text{and} \quad N^{mol} \propto \mathcal{N}^{6.6}. \tag{13}$$

This implies that, as we go to smaller systems (smaller $\mathcal{N}$), the difference in the predictions tend to quickly disappear. This trend will not be changed during the evolution of the hadron gas, which, as shown in Fig. 5, only produces mild changes in the multiplicities.

Using the initial conditions, we integrate the evolution equation (2) and stop at the kinetic freeze-out time, τ_F, given by (8) (and thus carrying another $\mathcal{N}$ dependence).

Following this procedure, we can replot Fig. 5 in terms of the variable $\mathcal{N}$. We show the new plots in Figs. 6(a) and 6(b) for the T_{cc}^+ and $X(3872)$, respectively. We observe that, not surprisingly, both tetraquark and molecule multiplicities increase as the system size grows. However, the number of molecules increases much more. This suggests that collisions with heavier ions are really more useful to discriminate between the two configurations.

The ratio between the T_{cc}^+ and $X(3872)$ abundances, shown in Fig. 6(c), has a very interesting behavior. In order to form a $X(3872)$, we need to produce one $c - \bar{c}$ pair. On the other hand, the formation of one T_{cc}^+ requires the production of two $c - \bar{c}$ pairs. Therefore, in collisions of small systems, one would expect the ratio $T_{cc}^+/X(3872)$ to be roughly one half. Moving to larger systems, due to the interactions with the medium, this difference tends to decrease, and the ratio tends to grow. This is what we see in tetraquark curve in Fig. 6(c). For tetraquarks, we can make predictions of the final yields based almost only on the initial conditions. This is so because, as one can see in Fig. 5, the tetraquark abundances almost do not change during the evolution of the hadron gas. In the molecular approach, the initial ratio is strongly affected by the powers of the binding energies, which are different for T_{cc}^+ and $X(3872)$. Moreover, in this case, the evolution plays a more important role, depending on the details of the interactions which are different for T_{cc}^+ and $X(3872)$. The outcome of all these dependences is the falling curve in Fig. 6(c). This result suggests that the behavior of the $T_{cc}^+/X(3872)$ ratio might be useful to discriminate between tetraquarks and molecules. The subject deserves further studies.

These results are predictions that can be tested experimentally in the future.

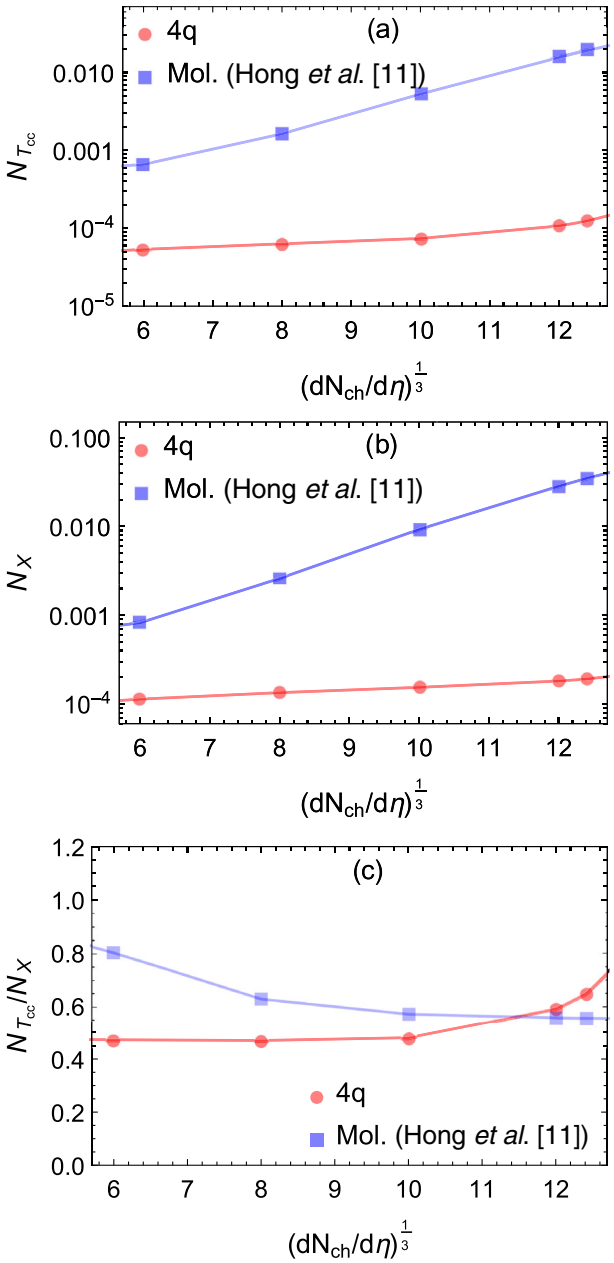

FIG. 6. (a) The T_{cc} abundance as a function of $[dN/d\eta(\eta=0)]^{1/3}$, with initial conditions given by the coalescence model. (b) Same as (a) but for the $X(3872)$ state. (c) The ratio between the T_{cc} and $X(3872)$ abundances as a function of $[dN/d\eta(\eta=0)]^{1/3}$, with initial conditions given by the coalescence model.

V. CONCLUSIONS

In this work, we have investigated the multiplicity evolution of the doubly charmed state T_{cc}^{+} in a hot hadron gas produced in the late stage of heavy-ion collisions. Effective Lagrangians have been used to calculate the thermal cross sections of T_{cc}^{+} production in reactions such as $T_{cc}^{+}\pi, T_{cc}^{+}\rho \to D^{(*)}D^{(*)}$ and its absorption in the corresponding inverse ones. We have found that the magnitude of the thermally averaged cross sections for the dissociation and production reactions differ in some cases by factors of some orders of magnitude.

With the thermal cross sections as input, we have solved the rate equation to determine the time evolution of the T_{cc}^{+} multiplicity, considering different internal structures in the context of the coalescence model: T_{cc}^{+} as a S-wave tetraquark produced via quark coalescence mechanism from the QGP phase at the critical temperature; and as a S-wave weakly bound hadronic molecule from the coalescence of mesons DD^{*} formed at the end of the mixed phase. The results have suggested that when the initial conditions from four-quark coalescence model are employed, $N_{T_{cc}}$ increases by a factor about 2 at freeze-out. However, it is still 2 order of magnitude smaller than the final yield of molecules formed from hadron coalescence. Therefore, we believe that the measurement of the T_{cc}^{+} abundance in HICs might help in discriminating one structure from the other. We emphasize that we presented for the first time a fair comparison between a "pure" molecule evolution and a "pure" tetraquark evolution through the hadronic medium in the context of the Effective Lagrangian approach. We also used here the connection between the time evolution of the hadronic fireball and the measured charged particle rapidity density (measured at midrapidities). Both for molecules and tetraquarks the multiplicities increase with $[dN/d\eta(\eta = 0)]$.

Using the phenomenological relations involving $\mathcal{N}$, we were able arrive at the predictions shown in Fig. 6, which can be compared to data, when they will be available. Our results are encouraging. They suggest that it is indeed possible to use heavy ion collisions to determine the internal structure of the new heavy exotic states. We plan in the near future to carry out these calculations in a more rigorous way, improving, among other things, our techniques to estimate the relevant volumes.

ACKNOWLEDGMENTS

The authors would like to thank the Brazilian funding agencies for their financial support: CNPq (LMA: Contracts No. 309950/2020-1 and No. 400546/2016-7), FAPESB (LMA: Contract No. INT0007/2016) and INCT-FNA.

[1] R. Aaij *et al.* (LHCb Collaboration), Nat. Phys. **2022**, 1 (2022).
[2] R. Aaij *et al.* (LHCb Collaboration), Nat. Commun. **13**, 3351 (2022).
[3] B. A. Gelman and S. Nussinov, Phys. Lett. B **551**, 296 (2003).
[4] D. Janc and M. Rosina, Few Body Syst. **35**, 175 (2004).
[5] J. Vijande, F. Fernandez, A. Valcarce, and B. Silvestre-Brac, Eur. Phys. J. A **19**, 383 (2004).
[6] F. S. Navarra, M. Nielsen, and S. H. Lee, Phys. Lett. B **649**, 166 (2007).
[7] J. Vijande, E. Weissman, A. Valcarce, and N. Barnea, Phys. Rev. D **76**, 094027 (2007).
[8] D. Ebert, R. N. Faustov, V. O. Galkin, and W. Lucha, Phys. Rev. D **76**, 114015 (2007).
[9] S. H. Lee and S. Yasui, Eur. Phys. J. C **64**, 283 (2009).
[10] Y. Yang, C. Deng, J. Ping, and T. Goldman, Phys. Rev. D **80**, 114023 (2009).
[11] J. Hong, S. Cho, T. Song, and S. H. Lee, Phys. Rev. C **98**, 014913 (2018).
[12] R. J. Hudspith, B. Colquhoun, A. Francis, R. Lewis, and K. Maltman, Phys. Rev. D **102**, 114506 (2020).
[13] J. B. Cheng, S. Y. Li, Y. R. Liu, Z. G. Si, and T. Yao, Chin. Phys. C **45**, 043102 (2021).
[14] Q. Qin, Y. F. Shen, and F. S. Yu, Chin. Phys. C **45**, 103106 (2021).
[15] S. S. Agaev, K. Azizi, and H. Sundu, Nucl. Phys. **B975**, 115650 (2022).
[16] X. K. Dong, F. K. Guo, and B. S. Zou, Commun. Theor. Phys. **73**, 125201 (2021).
[17] Y. Huang, H. Q. Zhu, L. S. Geng, and R. Wang, Phys. Rev. D **104**, 116008 (2021).
[18] N. Li, Z. F. Sun, X. Liu, and S. L. Zhu, Chin. Phys. Lett. **38**, 092001 (2021).
[19] H. Ren, F. Wu, and R. Zhu, Adv. High Energy Phys. **2022**, 9103031 (2022).
[20] Q. Xin and Z. G. Wang, arXiv:2108.12597.
[21] G. Yang, J. Ping, and J. Segovia, Phys. Rev. D **104**, 094035 (2021).
[22] L. Meng, G. J. Wang, B. Wang, and S. L. Zhu, Phys. Rev. D **104**, L051502 (2021).
[23] X. Z. Ling, M. Z. Liu, L. S. Geng, E. Wang, and J. J. Xie, Phys. Lett. B **826**, 136897 (2022).
[24] S. Fleming, R. Hodges, and T. Mehen, Phys. Rev. D **104**, 116010 (2021).
[25] Y. Jin, S. Y. Li, Y. R. Liu, Q. Qin, Z. G. Si, and F. S. Yu, Phys. Rev. D **104**, 114009 (2021).
[26] K. Azizi and U. Özdem, Phys. Rev. D **104**, 114002 (2021).
[27] Y. Hu, J. Liao, E. Wang, Q. Wang, H. Xing, and H. Zhang, Phys. Rev. D **104**, L111502 (2021).

[28] L. M. Abreu, F. S. Navarra, M. Nielsen, and H. P. L. Vieira, Eur. Phys. J. C **82**, 296 (2022).
[29] L. R. Dai, R. Molina, and E. Oset, arXiv:2110.15270.
[30] M. Albaladejo, Phys. Lett. B **829**, 137052 (2022).
[31] L. W. Chen, C. M. Ko, W. Liu, and M. Nielsen, Phys. Rev. C **76**, 014906 (2007); F. Carvalho, F. O. Duraes, F. S. Navarra, and M. Nielsen, Phys. Rev. C **72**, 024902 (2005); B. Osorio Rodrigues, M. E. Bracco, M. Nielsen, and F. S. Navarra, Nucl. Phys. **A852**, 127 (2011).
[32] S. Cho and S. H. Lee, Phys. Rev. C **88**, 054901 (2013);
[33] A. Martinez Torres, K. P. Khemchandani, F. S. Navarra, M. Nielsen, and L. M. Abreu, Phys. Rev. D **90**, 114023 (2014); Acta Phys. Pol. B Proc. Suppl. **8**, 247 (2015).
[34] L. M. Abreu, K. P. Khemchandani, A. Martinez Torres, F. S. Navarra, and M. Nielsen, Phys. Lett. B **761**, 303 (2016).
[35] L. M. Abreu, K. P. Khemchandani, A. Martinez Torres, F. S. Navarra, M. Nielsen, and A. L. Vasconcellos, Phys. Rev. D **95**, 096002 (2017).
[36] A. Martínez Torres, K. P. Khemchandani, L. M. Abreu, F. S. Navarra, and M. Nielsen, Phys. Rev. D **97**, 056001 (2018).
[37] L. M. Abreu, K. P. Khemchandani, A. Martínez Torres, F. S. Navarra, and M. Nielsen, Phys. Rev. C **97**, 044902 (2018).
[38] L. M. Abreu, F. S. Navarra, and M. Nielsen, Phys. Rev. C **101**, 014906 (2020).
[39] C. Le Roux, F. S. Navarra, and L. M. Abreu, Phys. Lett. B **817**, 136284 (2021).
[40] P. Koch, B. Muller, and J. Rafelski, Phys. Rep. **142**, 167 (1986).
[41] L. M. Abreu, F. S. Navarra, M. Nielsen, and A. L. Vasconcellos, Eur. Phys. J. C **78**, 752 (2018).
[42] L. M. Abreu, Phys. Rev. D **103**, 036013 (2021).
[43] S. Cho *et al.* (ExHIC Collaboration), Prog. Part. Nucl. Phys. **95**, 279 (2017).
[44] B. Abelev *et al.* (ALICE Collaboration), Phys. Rev. C **88**, 044910 (2013).
[45] Y. Hama and F. S. Navarra, Z. Phys. C **53**, 501 (1992).
[46] V. Vovchenko, B. Dönigus, and H. Stoecker, Phys. Rev. C **100**, 054906 (2019).
[47] H. Niemi, K. J. Eskola, R. Paatelainen, and K. Tuominen, Phys. Rev. C **93**, 014912 (2016).
[48] J. Adam *et al.* (ALICE Collaboration), J. High Energy Phys. 09 (2015) 148.